Electronic Supporting Information Available

Efficient white polymer light-emitting diodes (WPLEDs) based on covalent-grafting of $[Zn_2(MP)_3(OAc)]$ into PVK

Guorui Fu,[a,#] Yani He,[a,#] Wentao Li,[a] Tiezheng Miao,[a] Xingqiang Lü,*[a] Hongshan He,[b] Li Liu*[c] and Wai-Yeung Wong*[d]

Supporting information

Materials and methods

Reagents and solvents were received from Sigma Aldrich and used without further purification. All solvents, unless otherwise stated were degassed and stored over 3 Å activated molecule sieves prior to use. All manipulations of air and water sensitive compounds were carried out under a dry N_2atmosphere using the standard Schlenk line technique.

Elemental analyses were performed on a Perkin-Elmer 240C elemental analyzer. Fourier Transform Infrared (FT-IR) spectra were recorded on a Nicolet Nagna-IR 550 spectrophotometer in the region 4000-400 cm^{-1} using KBr pellets. ^1H NMR spectra were recorded on a JEOL EX 400 spectrometer with $SiMe_4$ as internal standard in DMSO-$d_6$at room temperature. ESI-MS was performed on a Finnigan LCQ^{DECA} XP HPLC-MS$_n$ mass spectrometer with a mass to charge (*m/z*) range of 4000 using a standard electro-spray ion source and MeCN as the solvent. Electronic absorption spectra for the solutions in the UV-visible region were recorded with a Cary 300 UV spectrophotometer. Visible emission and excitation spectra were collected by a combined fluorescence lifetime and steady-state spectrometer (FLS-980, Edinburgh) with a 450 W Xe lamp. Excited-state decay times were obtained by the same spectrometer but with a μF900 Xe lamp. The luminescent absolute quantum yield (Φ_{em}) in solution or solid-state was also measured by the same spectrometer using a 450 W Xe lamp and an integrating sphere. Gel permeation chromatography (GPC) analyses of polymers were performed using a Waters 1525 binary pump coupled to a Waters 2414 refractive index detector with HPLC THF as the eluant on America Polymer Standard linear mixed bed packing columns (particle size, 10 μm). GPC was calibrated using polystyrene standards. X-ray photoelectron spectroscopy (XPS) was carried out on a PHI 5700 XPS system equipped with a dual Mg X-ray source and monochromatic Al X-ray source complete with depth profile and angle-resolved capabilities. Powder X-ray diffraction (PXRD) patterns were recorded on a D/Max-IIIA diffractometer with graphite-monochromatized Cu Kα radiation (λ = 1.5418 Å).Thermal properties were characterized using thermogravimetric (TG) and differential scanning calorimetric (DSC) analyses on a NETZSCH TG 209 instrument under flowing nitrogen at a heating rate of 10 °C/min. The atomic force microscopy (AFM) images were measured on a NT-MDT Atomic Force Microscope NEXT. The Zn^{2+} distribution and the and the surface morphology of the polymeric film were recorded on a JSM-6330F field emission scanning electron microscope (SEM), operating at 3.0 kV with an energy dispersive X-ray spectrometry (EDS; BRUKER AXS, Microanalysis GMBH, Berlin, Germany).

Synthesis of the vinyl-modified organic precursor NAPMA (*N*-(2-

aminophenyl)methacrylamide)

To a stirred solution of THF (20 mL) cooled in ice-water bath, *o*-phenylenediamine (2.70 g, 25 mmol) and triethylamine (TEA; 3.00g, 30 mmol) were added, and the reaction mixture was continuously stirred at room temperature for 2 h. Another solution of THF (15 mL) containing methacryloyl chloride (2.61 g, 25 mmol) was added dropwise within 30 min, and the mixture was continuously stirred overnight under a N_2 atmosphere at room temperature. After removing all the insoluble salt by filtration, the THF solvent was distilled under reduced pressure. The residual was extracted with CH_2Cl_2 (30 mL), then the solution was washed with saturated saline for three times, and dried over anhydrous $MgSO_4$. After removal of the solvents under reduced pressure, the solid residual was purified with silica column chromatography using ethyl acetate/hexane (V/V = 3:1) as the eluent, affording to a white microcrystalline solid as desired. Yield: 1.75 g, 40%. Calc. for $C_{10}H_{12}N_2O$: C, 69.82; H, 6.92; N, 14.80%. Found: C, 69.74; H, 7.03; N, 14.71%. FT-IR (KBr, cm^{-1}): 3669 (w), 3270 (w), 2988 (w), 2376 (w), 1739 (w), 1660 (m), 1632 (m), 1596 (w), 1514 (s), 1443 (s), 1376 (w), 1328 (w), 1299 (w), 1262 (w), 1169 (m), 1060 (w), 1047 (w), 935 (m), 807 (w), 765 (vs), 675 (w), 638 (w), 576 (w), 512 (w). ^{1}H NMR (400 MHz, DMSO-d_6): δ (ppm) 9.15 (s, 1H, -NH-C=O-), 7.08 (d, 1H, -Ph), 6.94 (t, 1H, -Ph), 6.74 (d, 1H, -Ph), 6.56 (t, 1H, -Ph), 5.84 (s, 1H, =CH_2), 5.47 (s, 1H, =CH_2), 4.81 (s, 2H, -NH_2), 1.96 (s, 3H, -CH_3).

Synthesis of the vinyl-modified Schiff-base ligand HMP ((*E*)-*N*-(2-(2-hydroxy-3-methoxybenzylideneamino)phenyl)methacrylamide)

To a stirred solution of **NAPMA** (0.881 g, 5 mmol) in absolute EtOH (40 mL), an equimolar amount of solid 2-hydroxy-3-methoxy-benzaldehyde (0.761 g, 5 mmol) was added, and the resulting mixture was refluxed under an N_2 atmosphere for 4 h. After cooling to room temperature, the resultant yellow solution was filtered and left to stand for several days to obtain a yellow polycrystalline product. Yield: 1.163 g, 75%. Calc. for $C_{18}H_{18}N_2O_3$: C, 69.66; H, 5.85; N, 9.03%.Found: C, 69.89; H, 5.80; 9.08%. FT-IR (KBr, cm^{-1}): 3751 (w), 3307 (w), 3305 (w), 2971 (w), 2343 (w), 1662 (w), 1596 (m), 1485 (m), 1452 (s), 1328 (w), 1224 (w), 1077 (w), 932(m), 746 (vs), 670 (w), 638 (w), 569 (w), 510 (w). ^1H NMR (400 MHz, DMSO-d_6): δ (ppm) 12.71 (s, 1H, -OH), 9.49 (s, 1H, -NH-C=O-), 8.92 (s, 1H, -CH=N), 7.69 (m, 1H, -Ph), 7.44 (m, 1H, -Ph), 7.29 (m, 3H, -Ph), 7.14 (t, 1H, -Ph), 6.92 (m, 1H, -Ph), 5.77 (d, 1H, =CH_2), 5.53 (d, 1H, =CH_2), 3.84 (s, 3H, -OCH_3), 1.95 (s, 3H, -CH_3). ESI-MS (in MeCN) *m/z*: 311.14 (100%), $[M+H]^+$.

Synthesis of the *tris*-vinyl-functionalized Zn^{2+}-complex monomer $[Zn_2(MP)_3(OAc)]$

To a stirred solution of the vinyl-modified Schiff-baseligand **HMP** (0.460 g, 1.5 mmol) in absolute EtOH (10 mL), an equimolar amount of solid NaOH (0.060 g, 1.0mmol) was added, and the resulting mixture was stirred at room temperature for 2 h. Another solution of $Zn(OAc)_2 \cdot 2H_2O$ (0.218 g mg, 1.0mol) in absolute EtOH (6 mL) was added, and the resultant mixture was refluxed under an N_2 atmosphere for 3 h. After cooling to room temperature, the clear yellow solution was filtered and left to stand for several days to obtain yellow microcrystalline product. Yield: 0.335 g, 60%. Calc. for $C_{56}H_{54}N_6O_{11}Zn_2$: C, 60.17; H, 4.87; N, 7.52%. Found: C, 60.15; H, 4.86; N, 7.58%. FT-IR (KBr, cm^{-1}): 3052 (w), 2933 (w), 2322 (w), 1673 (w), 1599 (m), 1538 (w), 1482 (m), 1447 (s), 1385 (m), 1335 (m), 1235 (m), 1188 (s), 1159 (m), 1074 (w), 1026 (w), 958 (w), 927 (w), 841 (m), 742 (s), 714 (vs), 622 (w), 579 (w), 529 (w). ^1H NMR (400 MHz, DMSO-d_6): δ (ppm) 9.53 (s, 3H, -NH-C=O), 8.36 (s, 3H, -CH=N), 7.71 (s, 3H, -Ph), 7.22 (m, 12H, -Ph), 6.88 (s, 3H, -Ph), 6.45 (s, 3H, -Ph), 5.75 (d, 3H, $=CH_2$), 5.52 (d, 3H, $=CH_2$), 3.83 (s, 9H, $-OCH_3$), 1.97 (s, 9H, $-CH_3$), 1.79 (s, 3H, -OAc). ESI-MS (in MeCN) *m/z*: 1117.25 (100%), $[M+H]^+$; 1057.23 (21%), $[M-(OAc)]^+$.

X-ray crystallography

Single crystals for complex **$[Zn_2(MP)_3(OAc)]$**$\cdot EtOH\cdot H_2O$ of suitable dimensions were mounted onto thin glass fibers. All the intensity data were collected on a Bruker SMART CCD diffractometer (Mo-Kα radiation and λ = 0.71073 Å) in Φ and ω scan modes. Structures were solved by Direct methods followed by difference Fourier syntheses, and then refined by full-matrix least-squares techniques against F^2 using SHELXTL.[1] All other non-hydrogen atoms were refined with anisotropic thermal parameters. Absorption corrections were applied using SADABS.[2] All hydrogen atoms were placed in calculated positions and refined isotropically using a riding model. Crystallographic data, relevant atomic distances and bond angles for complex **$[Zn_2(MP)_3(OAc)]$**$\cdot EtOH\cdot H_2O$ are presented in Tables S1-2, respectively. CCDC number 1894830 for complex **$[Zn_2(MP)_3(OAc)]$**$\cdot EtOH\cdot H_2O$.

Electronic Structure Calculations

Theoretical studies on the electronic structure for the complex monomer **$[Zn_2(MP)_3(OAc)]$** were carried out using density functional theory (DFT) and time-dependent DFT (TD-DFT) methods. The molecular structure was optimized at the ground state (S_0) in the gas phase. DFT calculations were conducted with the popular B3LYP functional theory. The 6-31G (d,p) basis set was applied for C, H, N, O, atoms, while effective core potentials employed for Zn atom were based on a LanL2DZ basis set.[3-4] The excited states' energies were computed by TD-DFT based on the ground-state (S_0) geometry. Additionally, the natural transition orbital (NTO) was analyzed for $S_0 \rightarrow T_1$ excitation based on the first triplet state (T_1) geometry optimized by UB3LYP. All calculations were carried out with Gaussian 09, Revision D.01 software package.[5] The electron density diagrams of molecular orbitals were obtained with the ChemOffice 2010 graphics program.

Synthesis of the AIBN-initiated PVK (poly(*N*-vinyl-carbazole)

The homogeneous polymerization of in activation with AIBN for comparison was carried out in a Fisher-Porter glass reactor and protected by nitrogen according to the typical procedure. To a solution of N-vinyl-carbazole (NVK, 3.67 g, 19 mmol) in dry 1,2-dichlorobenzene (15 mL), AIBN initiator (46.8 mg, 1.5 mol% of NVK) was added, and the resultant homogeneous solution was purged with N_2 for 10 min and sealed under a reduced N_2 atmosphere. The mixture was heated to 80 °C with continuous stirring for 48 h. The viscous mixture was diluted with dry 1,2-dichlorobenzene (15 mL) and precipitated with absolute diethyl ether (50 mL) three times. The resulting solid PVK was collected by filtration and dried at 45 °C under vacuum to constant weight. For PVK: Yield: 90%. FT-IR (KBr, cm^{-1}): 3074 (w), 3022 (w), 2969 (w), 2927 (w), 1623 (w), 1481 (m), 1450 (vs), 1406 (w), 1321 (s), 1220 (m), 1154 (m), 1124 (w), 1092 (w), 1031 (w), 1001 (w), 924 (w), 744 (s), 719 (s), 656 (w), 614 (w), 572 (w), 476 (w). ^1H NMR (400 MHz, DMSO-d_6): δ (ppm) 8.25-3.95 (b, 8H), 2.15-3.95 (b, 1H), 2.15-0.5 (b, 2H).

Synthesis of the [$Zn_2(MP)_3(OAc)$]-grafted polymeric films Poly(NVK-*co*-[$Zn_2(MP)_3(OAc)$]) with different feedings (100:1, 200:1, 300:1, 400:1 and 500:1)

A mixture of NVK and the complex monomer **[$Zn_2(MP)_3(OAc)$]** at a stipulated feed molar ratio (100:1, 200:1, 300:1, 400:1 or 500:1) in the presence of AIBN (1.5 mol% of NVK) was dissolved in dry 1,2-dichlorobenzene (30 mL), and the resultant homogeneous solution was purged with N_2 for 10 min and sealed under a reduced N_2 atmosphere. The mixture was heated to 80 °C with continuous stirring for 48 h. The viscous mixture was diluted with dry 1,2-dichlorobenzene (15 mL) and precipitated with absolute diethylether (50 mL) three times. The resulting solid products were collected by filtration and dried at 45 °C under vacuum to constant weight, respectively. Further dissolving one of the obtained solid products in absolute toluene (10 mL) at a concentration of 5 mg/mL, and then spin-coating at 3000 rpm on a clean quartz slide and finally drying in air, the almost similar film thickness of 40 nm was measured by ellipsometry through collecting data every 5° from 65° to 75° and fitted using a Cauchy film on a gold model.

For polymeric films **Poly(NVK-*co*-[$Zn_2(MP)_3(OAc)$])** (100:1; 200:1, 300:1, 400:1 or 500:1): Yield: 98% (100:1); 97% (200:1); 97% (300:1), 97% (400:1); 98% (500:1). Representative (200:1) FT-IR (KBr, cm^{-1}): 3056 (w), 2939 (w), 1675 (w), 1630 (m), 1597 (m), 1483 (m), 1450 (s), 1406 (w), 1325 (m), 1157 (m), 1126 (m), 1057 (w), 1026 (w), 1002 (w), 954 (w), 924 (w), 839 (w), 745 (vs), 720 (s), 615 (w), 586 (w), 514 (w), 479 (w), 434 (w). Representative (200:1) ^1H NMR (400 MHz, DMSO-d_6): δ (ppm) 9.01 (m, 3H, -NH-C=O), 8.58-5.93 (b, 770H+30H), 4.39-3.80 (b, 194H), 2.32 (d, 9H), 2.12-0.52 (b, 388H+12H).

Cyclic voltammetry (CV) measurement

CV measurement was performed on a computer-controlled EG&G Potentiostat/Galvanostat model 283 at RT with a conventional three-electrode cell using a an Ag/AgNO$_3$ (0.1 M) reference electrode, Pt carbon working electrode of 2 mm in diameter, and a platinum wire counter electrode. CV of the sample was performed in nitrogen-saturated dichloromethane containing 0.1 M Bu$_4$NPF$_6$ as supporting electrolyte. The CV was measured at a scan rate of 100 mV·s^{-1}. The HOMO and the LUMO energy levels of each complex are calculated according to the following equations,[6] $E_{\mathrm{HOMO}} = -(E_{\mathrm{OX}}{}^{\mathrm{on}} + 4.8)$ eV, $E_{\mathrm{LUMO}} = E_{\mathrm{HOMO}} + E_{\mathrm{g}}{}^{\mathrm{OPT}}$ eV, and where $E_{\mathrm{OX}}{}^{\mathrm{on}}$ is the recorded onset oxidation potential of the complex, and $E_{\mathrm{g}}{}^{\mathrm{OPT}}$ is the energy band gap estimated from the low-energy edge of the absorption spectra from the samples. The HOMO and LUMO energy levels for the other used materials were obtained from the literatures.[7]

WPLEDs' fabrication and testing based on polymeric film Poly(NVK-*co*-[Zn$_2$(MP)$_3$(OAc)]) (200:1)

Each of the **WPLEDs-I-II** was fabricated on ITO (Indium tin oxide) coated glass substrates with a sheet resistance of 20Ω per square. Patterned ITO coated glass substrates were washed with acetone, detergent, D. I. water and isopropanol in an ultrasonic bath. After being exposed under oxygen plasma for 20 min, PEDOT:PSS from water solution was spin-coated (at 2000 rpm) on the substrate and followed by drying in a vacuum oven at 140 °C for 20 min, giving a film of 40 nm thickness. The THF solution (20 mg/mL) of the polymer **Poly(NVK-*co*-[Zn$_2$(MP)$_3$(OAc)])** (200:1)as the emitting layer was prepared under an N$_2$

atmosphere and spin-coated (at 4000 rpm) on the PEDOT:PSS layer with a thickness of 40 nm. The TPBi layer (30 nm) was thermally deposited onto the emitting layer especially for **WPLED-I**. Finally, a thin layer (1 nm) of LiF followed by 100 nm thickness Al capping layer was deposited onto the substrate under vacuum of 5×10^{-6} Pa. The typical active area of the four devices is 9 mm^2. Current density (J)-voltage (V)-luminance (L) was collected using a Keithley 2400 source meter equipped with a calibrated silicon photodiode. The electroluminescent spectra were measured by a PR655 spectrometer. The eternal quantum efficiency (η_{EQE}) values were determined by a Si photodiode with calibration in an integration sphere (IS080, Labsphere).

References

1.G. M.Sheldrick, *SHELXL-97*, Program for Crystal Structure Refinement, University of Göttingen, Göttingen, Germany, 1997.

2. G. M. Sheldrick, *SADABS*, University of Göttingen, Göttingen, Germany, 1996.
3. W. R. Wadt, P. J. Hay, Ab initio effective core potentials for molecular calculations, potentials for main group elements Na to Bi. *J. Chem. Phys.* 1985, **82**, 284-298.
4. P. J. Hay, W. R. Wadt, Ab initio effective core potentials for molecular calculations,potentials for K to Au Including the outermost core orbitals. *J. Chem. Phys.* 1985, **82**, 299-310.
5. Gaussian 09, Revision D.01, M. J. Frisch, G. W. Trucks, H. B. Schlegel, G. E. Scuseria, M. A. Robb, J. R. Cheeseman, G. Scalmani, V. Barone, B. Mennucci, G. A. Petersson, H. Nakatsuji, M. Caricato, X. Li, H. P. Hratchian, A. F. Izmaylov, J. Bloino, G. Zheng, J. L.

Sonnenberg, M. Hada, M. Ehara, K. Toyota, R. Fukuda, J. Hasegawa, M. Ishida, T. Nakajima, Y. Honda, O. Kitao, H. Nakai, T. Vreven, J. A. Montgomery, Jr., J. E. Peralta, F. Ogliaro, M. Bearpark, J. J. Heyd, E. Brothers, K. N. Kudin, V. N. Staroverov, R. Kobayashi, J. Normand, K. Raghavachari, A. Rendell, J. C. Burant, S. S. Iyengar, J. Tomasi, M. Cossi, N. Rega, J. M. Millam, M. Klene, J. E. Knox, J. B. Cross, V. Bakken, C. Adamo, J. Jaramillo, R. Gomperts, R. E. Stratmann, O. Yazyev, A. J. Austin, R. Cammi, C. Pomelli, J. W. Ochterski, R. L. Martin, K. Morokuma, V. G. Zakrzewski, G. A. Voth, P. Salvador, J. J. Dannenberg, S. Dapprich, A. D. Daniels, Ö. Farkas, J. B. Foresman, J. V. Ortiz, J. Cioslowski, and D. J. Fox, Gaussian, Inc., Wallingford CT, 2009.

6. H. Y. Chen, C. T. Chen and C. T. Chen, *Macromolecules* 2010, **43**, 3613-3623.
7. E. Zysman-Colman, S. S. Ghosh, G. Xie, S. Varghese, M. Chowdhury, N. Sharma, D. B. Cordes, A. M. Z. Slawin and I. D. W. Samuel, *ACS Appl. Mater. & Interfaces* 2016, **8**, 9247-9253.

Table S1 Crystal data and structure refinement for the complex **$[Zn_2(MP)_3(OAc)]$**$\cdot EtOH\cdot H_2O$

Compound	**$[Zn_2(MP)_3(OAc)]$**$\cdot EtOH\cdot H_2O$
Empirical formula	$C_{58}H_{62}N_6O_{13}Zn_2$
Formula weight	1181.88
Crystal system	Monoclinic
Space group	*P2(1)/c*
a/Å	15.210(5)
b/Å	16.731(5)
c/Å	23.716(7)
α/°	90
β/°	104.529(6)
γ/°	90
V/Å^3	5842(3)
Z	4
ρ/g·cm^{-3}	1.344
Crystal size/mm	0.29× 0.20 × 0.17
μ(Mo-Kα)/mm^{-1}	0.888
Data/restraints/parameters	12396/0/712
Quality-of-fit indicator	0.908
No. unique reflections	12396
No. observed reflections	32860
Final R indices [$I > 2\sigma(I)$]	R_1 = 0.0801
	wR_2 = 0.2136
R indices (all data)	R_1 = 0.2183
	wR_2 = 0.2943

Table S2 Relevant atomic distances (Å) and bond angles (°) for the complex **[Zn_2(MP)$_3$(OAc)]**·EtOH·H_2O

Compound	**[Zn_2(MP)$_3$(OAc)]**·EtOH·H_2O		
Zn(1)-N(2)	2.008(6)	Zn(2)-N(5)	2.023(6)
Zn(1)-N(3)	2.087(6)	Zn(2)-O(4)	2.374(6)
Zn(1)-O(2)	1.935(5)	Zn(2)-O(5)	2.016(5)
Zn(1)-O(5)	1.995(5)	Zn(2)-O(8)	1.995(5)
Zn(1)-O(8)	2/375(5)	Zn(2)-O(10)	1.918(7)
C(2)-C(3)	1.357(13)	C(34)-C(35)	1.290(20)
C(52)-C(54)	1.314(14)	Zn(1)···Zn(2)	3.206(2)
N(2)-Zn(1)-N(3)	100.9(3)	N(5)-Zn(2)-O(4)	99.7(2)
N(2)-Zn(1)-O(2)	94.2(2)	N(5)-Zn(2)-O(5)	117.7(2)
N(2)-Zn(1)-O(5)	159.1(2)	N(5)-Zn(2)-O(8)	93.1(2)
N(2)-Zn(1)-O(8)	90.2(2)	N(5)-Zn(2)-O(10)	125.0(3)

Table S3 Photophysical properties of the complex monomer **$[Zn_2(MP)_3(OAc)]$**in solution and its grafting polymers **Poly(NVK-*co*-$[Zn_2(MP)_3(OAc)]$)** (100:1, 200:1, 300:1, 400:1 or 500:1) in solid-state film) at RT or 77 K

Sample	λ_{Abs} (nm)	λ_{ex}	λ_{em}(nm, τ)	CIE	CCT (K)/CRI
HMP[a]	232, 290, 368(sh)	306	430	-	-
$[Zn_2(MP)_3(OAc)]$[a]	230, 290, 352, 404, 414, 448	397[a]	538 (0.26 and 1.74 ns)[a]	0.487, 0.506	-
	-	432[b]	590 (0.63 and 2.12 μs)[b]	-	-
PVK[c]	-	272	418	-	-
Poly(NVK-*co*-$[Zn_2(MP)_3(OAc)]$)[c]			420, 540	-	-
100:1	-	315-345		0.396-0.441, 0.410-0.458	4553-5337/62-66
200:1	-	315-345		0.290-0.323, 0.319-333	8533-9494/74-75
300:1	-	315-345		0.258-0.265, 0.296-0.305	10790-12099/-
400:1	-	315-345		0.226-0.230, 0.229-0.249	-
500:1	-	315-345		0.205-0.208, 0.180-0.282	-

[a]In dilute MeCN solution at RT or 77 K [b]and [c]in solid-state film at RT.

Table S4 TD-DFT results of the complex monomer **[Zn$_2$(MP)$_3$(OAc)]** on the basis of its optimized S_0 geometry

		Contribn of metal d_π and π orbitals of ligand $d_\pi$to MOs (%)						Confign of $S_0 \rightarrow S_n$ excitation, λ_{cal}(nm)/f[a]	Confign of $S_0 \rightarrow T_1$ excitation, λ_{cal}(nm)[a]
Complex	MO	Zn1	Zn2	MP1	MP2	MP3	OAc$^-$		
[Zn$_2$(MP)$_3$(OAc)]	LUMO+2	0.17	0.46	17.91	1.13	80.21	0.12	$S_0 \rightarrow S_1$: HOMO → LUMO (91.06), 450, 0.0172; HOMO → LUMO+2 (5.93), 450, 0.0172 $S_0 \rightarrow S_2$: HOMO→LUMO+2, (76.37), 416; HOMO-1→LUMO(8.30), 416; HOMO→LUMO+1(5.20), 416; HOMO-2→LUMO (5.03), 416; HOMO→LUMO (3.23), 416 $S_0 \rightarrow S_3$: HOMO→LUMO+1, (89.73), 406; HOMO-1→LUMO(5.15), 406; HOMO→LUMO+2(2.15), 406	HOMO → LUMO (83.56), 593; HOMO → LUMO+2 (6.09), 593
	LUMO+1	0.26	0.11	1.45	95.44	2.73	0.01		
	LUMO	0.32	0.12	80.59	2.27	16.66	0.04		
	HOMO	0.26	0.14	82.76	0.40	16.27	0.18		
	HOMO-1	0.66	0.28	8.35	54.25	36.30	0.16		
	HOMO-2	0.67	0.41	7.31	38.68	52.00	0.93		

Table S5 NTO results of the complex monomer **$[Zn_2(MP)_3(OAc)]$** on the basis of its optimized T_1geometry

		Contribn of metal $d_\pi$orbitals and πorbitals of ligand to NTOs (%)					
complex	NTO	Zn1	Zn2	MP1	MP2	MP3	OAc^-
$[Zn_2(MP)_3(OAc)]$	Hole	0.45	0.06	95.21	0.38	3.87	0.03
	Partical	0.23	0.04	96.96	0.38	2.39	0.37

Table S6 GPC and XPS data of the grafting polymers **Poly(NVK-*co*-[$Zn_2(MP)_3(OAc)$])**(100:1, 200:1, 300:1, 400:1 or 500:1)

Sample	Feeding	$M_n{}^a$/g mol^{-1}	PDI^b	Grafting^c
PVK	-	26316	1.20	-
Poly(NVK-*co*-[$Zn_2(MP)_3(OAc)$])	100:1	17496	1.13	98:1
	200:1	34156	1.19	194:1
	300:1	50498	1.23	292:1
	400:1	67364	1.25	388:1
	500:1	82512	1.29	491:1

^{a}M_n is the number-average molecular weight. ^{b}PDI = M_w/M_n, where M_w is the weight-average molecular weight. ^{C}Grafting concentration is determined by XPS.

Table S7 Electroluminescent performance comparison of WOLEDs/WPLEDs based on specific organo-Zn^{2+}-chromophore from the literatures[16-20, 22-23] and **Poly(NVK-*co*-[Zn$_2$(MP)$_3$(OAc)])** in this work

WOLED/WPLED configuration	**White-light CIE**	V_{on}	L^{Max}	ηc^{Max}	η_p^{Max}	η_{EQE}^{Max}
	x, *y*	V	cd/m^2	cd/A	lm/W	%
ITO/PEDOT:PSS/**Poly(NVK-*co*-[Zn$_2$(MP)$_3$(OAc)])**/TPBi/LiF/Al	0.297-0.300, 0.332-0.339	7.0	44.2 (12.0 V)	2.2 (12.0 V)	1.0 (12.0 V)	1.7
ITO/PEDOT:PSS/**Poly(NVK-*co*-[Zn$_2$(MP)$_3$(OAc)])**/BCP/TPBi/LiF/Al	0.325-0.329, 0.300-0.310	6.0	46.2 (15.0 V)	13.0 (15.0 V)	6.1 (15.0 V)	9.2
ITO/α-NPD/DCM:**[Zn(hpc)$_2$]**/BCP/Alq$_3$/LiF/Al[16a]	0.26-0.27, 0.30-0.31	5.0	2210 (12.0 V)	1.23 (9.5 V)	0.44 (8.5 V)	-
ITO/PVK:TPD/**Zn(BTZ)$_2$**:rubrene/**Zn(BTZ)$_2$**/Mg:Ag[16b]	0.341, 0.334	-	4000	-	-	0.63
ITO/α-NPD/**Zn(hpb)$_2$**:Ir(btp)$_2$acac/BCP/Alq$_3$/LiF/Al[17]	0.34,0.27	5.0	3500 (15.0 V)	5.2 (11.5 V)	1.43 (11.5 V)	-
ITO/α-NPD/**[Zn(hpb)$_2$]**/**Zn(hpb)mq**/BCP/Alq$_3$/LiF/Al[18a]	0.29-0.31, 0.38-0.45	5.0	8390 (14.0 V)	-	-	-
ITO/PEDOT:PSS/NPB/**Zn(HPB)$_2$**/**Zn(HPB)q**/Alq$_3$/LiAl[18b]	0.26-0.32, 0.35-0.43	5.0	15171	1.65	-	0.7
ITO/PEDOT:PSS/NPB/**Zn(HPB)$_2$**/**Zn(HPQ)$_2$**/Al[19a]	0.262-0.338, 0.319-0.376	4.75	12000 (10.0 V)	-	-	-
ITO/2T-NATA/**TPAHQZn**/NPBX/BCP/Alq$_3$/LiF[19b]	0.318-0.339, 0.301-0.318	5.0	12930 (12.0 V)	2.66 (10.0 V)	-	-
ITO/NPB/**Zn(HPB)$_2$**/**Zn(HPB)$_2$**:DCJTB/Alq$_3$/LiF/Al[19c]	0.304-0.312, 0.332-0.359	-	-	-	-	-
ITO/NPB/BCP/**Zn(phen)q**/LiF/Al[19d]	0.26-.31, 0.33-0.42	-	5400	-	-	-
ITO/TPD/**Zn(BTZ)$_2$**/OXD-7/MgIn[19e]	0.246, 0.363	-	10190 (8.0 V)	-	0.89 (8.0 V)	-
ITO/MeOTPD:F$_4$-TCNQ/MeOTPD/TCTA:**Zn-Salen**/BCP/TPBi/LiF/Al[20a]	0.26-0.32, 0.29-0.35	4.7	815 (8.6 V)	0.60	0.45	-
ITO/MeOTPD:F$_4$-TCNQ/MeOTPD/**Zn-Salen**/BCP/TPBi/LiF/Al[20a]	0.19-0.42, 0.16-0.48	5.9	706 (11.8 V)	0.40	0.13	-
ITO/NPB/**Zn2(4-TfmBTZ)$_4$**/LiF/Al[20b]	0.29, 0.33	5.7	2657 (13.9 V)	1.47 (13.9 V)	-	-
ITO/NPB/**Zn(4-TfmBTZ)$_2$**/LiF/Al[20c]	0.29-0.32, 0.32-0.38	8.0	2445 (14.0 V)	1.39	-	-
ITO/TPD/**Zn(BTZ)$_2$**/Al[20d]	0.28-0.33, 0.31-0.33	-	-	-	-	-
ITO/PEDOT:PSS/TPD/**Zn(BZT)$_2$**//Al[20e]	0.38, 0.40	9.1	-	-	-	-
ITO/TEDOT:PSS/PVK:**Zn(Salen)**/Ca/Al[22a]	0.32-0.43, 0.56-0.60	6.5	131 (16.0 V)	0.036 (14.5 V)	-	-
ITO/PEDOT:PSS/PVK/PVK:PBD:**Zn$_2$(AMOX)$_4$**/BCP/Alq$_3$/Al/Ag[22b]	-	-	-	1.12	0.30	-
ITO/PEDOT:PSS/PVK:OXD-7:**Zn-1**:Cu-3/3TPYMB/TPBi/LiF/Al[23]	0.35-0.42, 0.44	-	3150 (15.0 V)	14.67	6.58	6.88

Figure S1.^{1}H NMR spectra for the organic precursor **NAPAM**, the ligand **HMP**, the complex monomer **[Zn$_2$(MP)$_3$(OAc)], PVK** and the representative polymer **Poly(NVK-*co*-[Zn$_2$(MP)$_3$(OAc)])** (200:1) in DMSO-d_6 at RT.

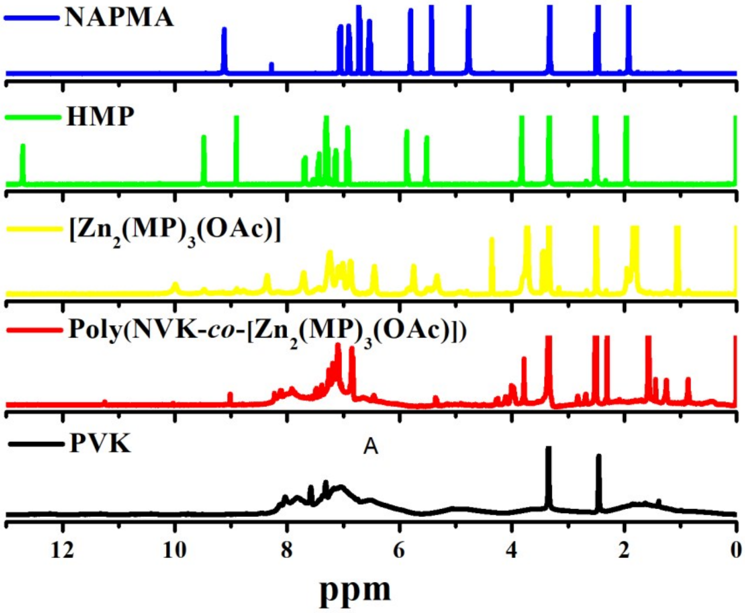

Figure S2. TG and DSC (inset) curves of the complex monomer **[Zn$_2$(MP)$_3$(OAc)], PVK** and the representative polymeric film **Poly(NVK-*co*-[Zn$_2$(MP)$_3$(OAc)])** (200:1).

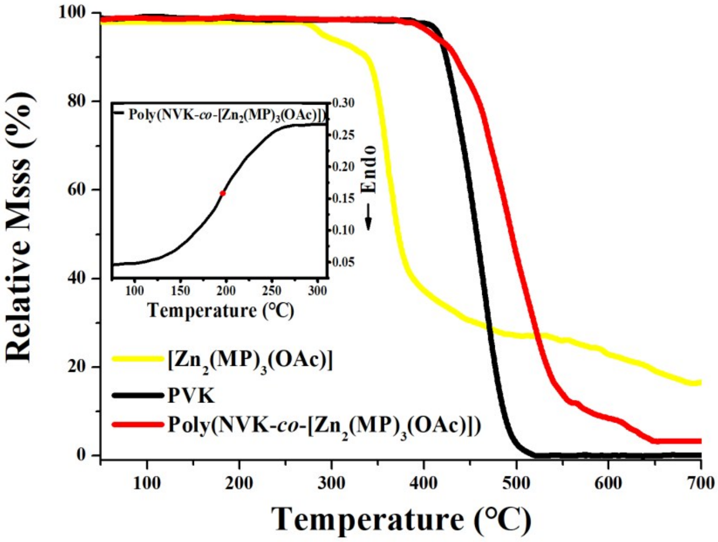

Figure S3. Normalized absorption and emission spectra of the ligand **HMP** and the complex monomer **[Zn$_2$(MP)$_3$(OAc)]** in solution at RT or 77 K.

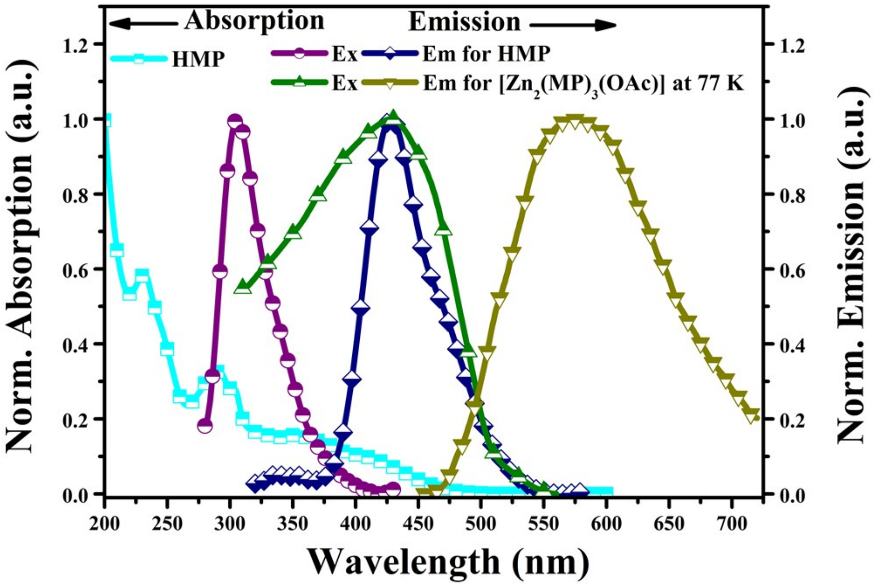

Figure S4. The normalized emission spectra (λ_{ex} = 397 nm) of the complex monomer **[Zn$_2$(MP)$_3$(OAc)]** under the same absorbance value at 397 nm in different solvents or solid-state at RT.

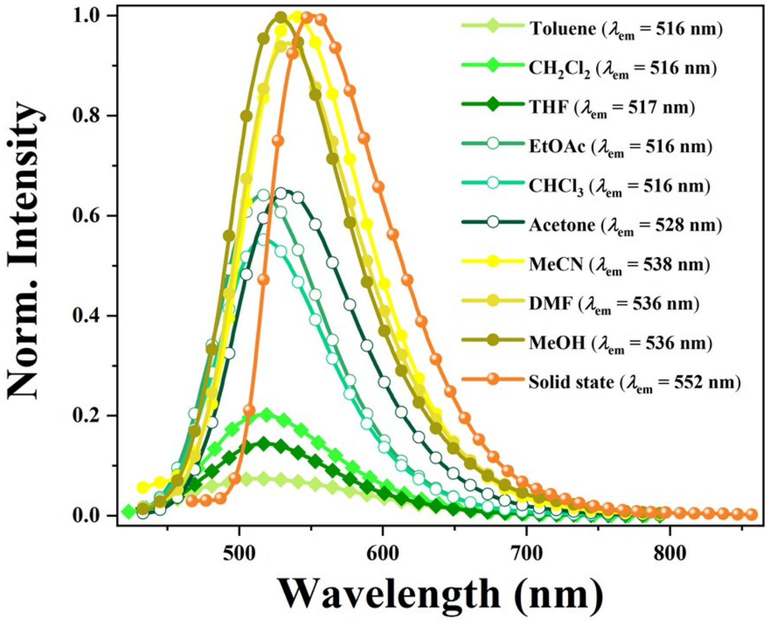

Figure S5. The NTO patterns for $S_0 \rightarrow T_1$ excitation for the complex monomer **[Zn$_2$(MP)$_3$(OAc)]** based on its optimized T_1 geometry.

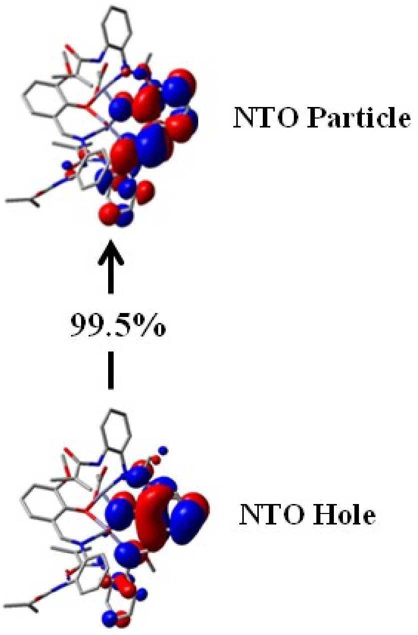

Figure S6. PXRD patterns of PVK and the representative polymeric film **Poly(NVK-*co*-[Zn$_2$(MP)$_3$(OAc)])** (200:1).

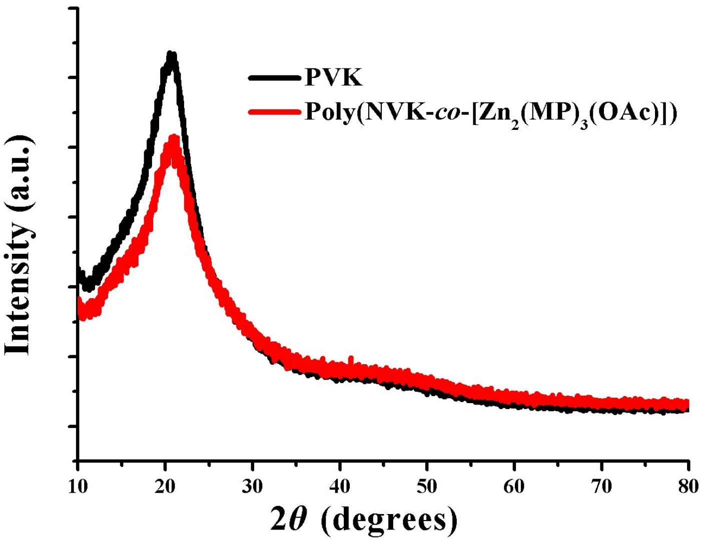

Figure S7. Normalized emission spectra and corresponding CIE chromatic coordinates (inset) of the polymeric films **Poly(NVK-*co*-[Zn_2(MP)$_3$(OAc)])** (100:1 (a); 300:1 (b); 400:1 (c) or 500:1 (d)) upon excitation (λ_{ex} = 315-345 nm) at RT.

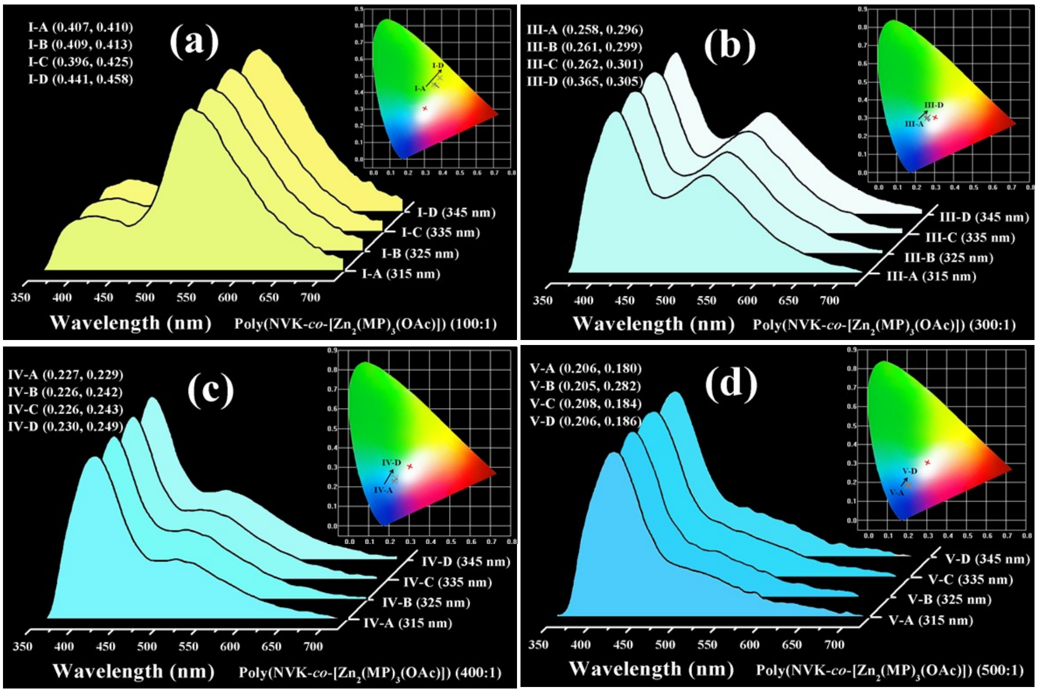

Figure S8. The AFM topographic images of the polymeric films **Poly(NVK-*co*-[Zn_2(MP)$_3$(OAc)])** (100:1 (a); 200:1 (b); 300:1 (c); 400:1 (d) or 500:1 (e)).

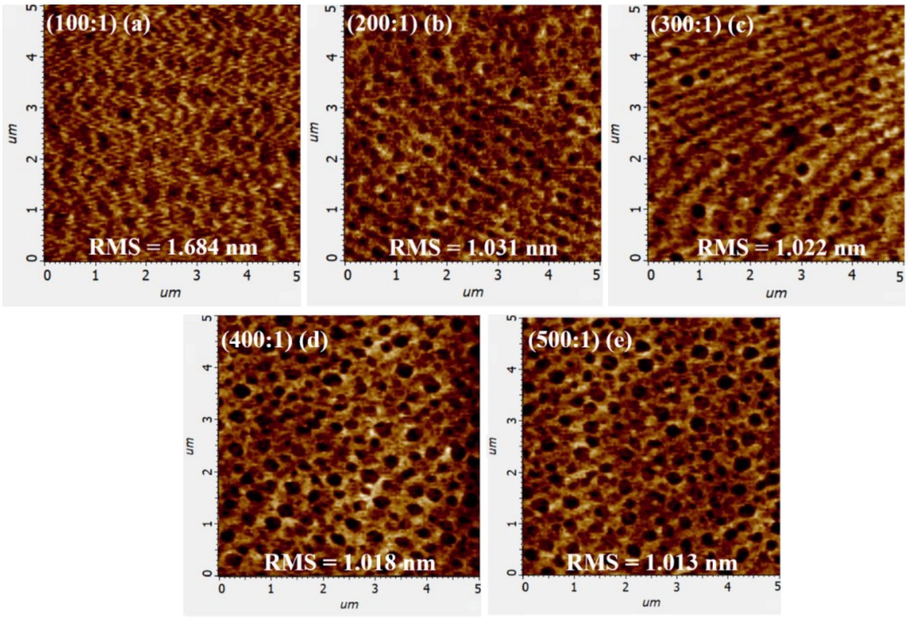

Figure S9. The SEM-EDS (1×10000; 5×10000; 6×10000; the EDS data) images of the representative polymeric film **Poly(NVK-*co*-[Zn_2(MP)$_3$(OAc)])** (200:1).

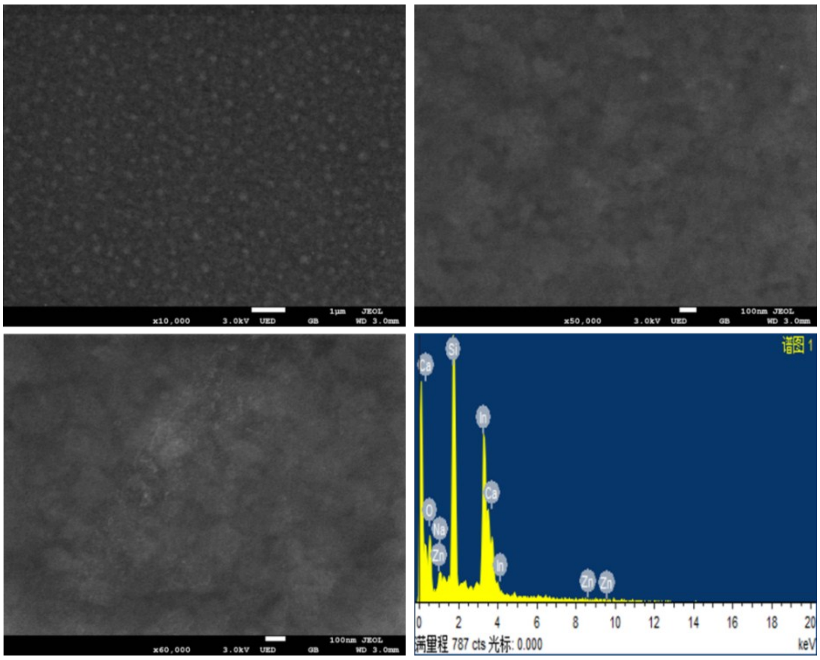

Figure S10. CV curve of the representative polymeric film **Poly(NVK-*co*-[Zn$_2$(MP)$_3$(OAc)])** (200:1) *versus* Fc$^+$/Fc in solution (scan rate = 100 mV/s).